

1 **SUPPLEMENTAL MATERIAL**

2

3 **SUPPLEMENTAL METHODS**

4 *Immune Profiling Cohort*

5 The *Immune Trajectory Cohort* consisted of preterm infants enrolled in the IRoN
6 (Immunoregulation of the Newborn) study conducted at the Department of Pediatrics,
7 University Hospital of Lübeck. Data were collected from infants born between October 1, 2014,
8 and December 31, 2024. Inclusion criteria were preterm birth (<37+0 weeks of gestation), in-
9 hospital treatment, and availability of lymphocyte subset analysis in peripheral blood within the
10 first 49 days of life (n = 511). Exclusion criteria included chromosomal abnormalities,
11 syndromal diseases, or death prior to hospital discharge (n = 12).

12 *Extended Phenotyping Cohort*

13 The *Extended Phenotyping Cohort* included preterm infants born at <32+0 weeks of gestation
14 and birth weight <1,500 g, enrolled in the IRoN study at the Department of Pediatrics,
15 University Hospital of Würzburg. Data were collected from infants born between January 1,
16 2022, and September 30, 2024 (n = 84). Exclusion criteria were the same as for the *Immune*
17 *Trajectory Cohort* (n = 6 infants excluded from analysis). Sampling of peripheral blood for flow
18 cytometric analysis occurred as early as possible after birth (median day: 3, range: 1-10) and
19 on day 28-30.

20 Baseline characteristics of both cohorts and major in-hospital complications related to
21 prematurity are detailed in Table 1.

22 **Definitions**

23 Gestational age (GA) was calculated from the best obstetric estimate according to early
24 prenatal ultrasound and obstetric examination. Small for gestational age (SGA) was defined
25 as a birth weight less than the 10th percentile according to sex-specific standards for birth
26 weight by postmenstrual age in Germany(1). Amniotic infection syndrome (or Triple I) was

27 suspected by the attending obstetrician as cause of preterm birth based on maternal fever plus
28 fetal tachycardia, a white blood cell count greater than 15 000/ μ L, or a foul-smelling discharge.
29 When chorionamnionitis was histologically confirmed it was considered as proven.

30 Neonatal sepsis was defined as blood culture-proven sepsis identified by clinical sepsis criteria
31 and detection of a causative pathogen in one or more blood cultures according to criteria of
32 the German National Nosocomial Infection Surveillance System in Preterm Infants (NEO-
33 KISS). Early-onset sepsis (EOS) was defined as sepsis occurring within the first 72 hours of
34 life, while late-onset sepsis (LOS) was defined as sepsis episode after 72 hours of life(2).

35 Bronchopulmonary dysplasia (BPD) was defined as requirement of supplemental oxygen
36 and/or ventilation support at 36 weeks' postmenstrual age(3). Intraventricular hemorrhage
37 (IVH) was diagnosed according to Papile classification based on cranial ultrasound findings(4).
38 Necrotizing enterocolitis (NEC) requiring surgery corresponded to clinical NEC classified as
39 Bell stage II or III with the need for laparotomy and macroscopic diagnosis of NEC(5). Focal
40 intestinal perforation (FIP) was defined as spontaneous intestinal perforation requiring
41 laparotomy or peritoneal drainage.

42 Ethics

43 Written informed consent was obtained from parents or legal representatives. The study
44 protocols were approved by the local ethics committees at the University of Lübeck (IRON AZ
45 15-304) and the University Hospital of Würzburg (IRON Würzburg 11/21 me). Blood samples
46 were obtained as part of routine clinical procedures, with additional volumes for research
47 purposes remaining below 1% of total blood volume per sampling, in compliance with
48 European Medicines Agency (EMA) guidelines on medicinal product investigation in preterm
49 and term neonates (PDCO, 2006).

50 Flow cytometry

51 Peripheral blood samples within both cohorts were collected in EDTA tubes and processed for
52 flow cytometry within 24 hours of collection.

53 Immune Profiling Cohort: Absolute and relative lymphocyte counts, including T helper cells and
54 cytotoxic T cells, B cells, and natural killer (NK) cells, were measured during routine centralized
55 laboratory diagnostics when blood samples were collected for clinical purposes. A BD
56 FACSCanto II system (BD Biosciences) equipped with the BD FACS Canto Clinical software
57 was used for analysis of lymphocyte subsets in whole blood utilizing Multitest 6-Color TBNK
58 (T cells and B cells) kits according to the manufacturer's protocols. Representative plots and
59 detailed information on the gating strategy used by the central laboratory are available in the
60 BD Biosciences user manual. Weekly checks of all cytometer performances were performed
61 using BD FACS 7-Color Setup Beads, with alternating use of BD Multi-Check Control and BD
62 Multi-Check CD4 Low Control quality controls twice daily.

63 Extended Phenotyping Cohort: Lymphocyte counts were determined as part of routine
64 diagnostics (ADVIA 2120i, Siemens Healthineers). Whole blood was stained with three
65 different antibody panels (Supplemental Table 2, Biolegend) for 30 minutes at room
66 temperature. Erythrocytes were lysed with FACS Lysing Solution (BD Biosciences), and cells
67 were washed, centrifuged (1,500 rpm, 5 min), and resuspended in PBS containing 0.5% BSA.
68 Data acquisition was performed on a BD FACSCanto II cytometer (BD Biosciences), and
69 analysis was conducted using FlowJo software (version 10; Tree Star). Regular checks of
70 cytometer performances were performed using 8 peak Rainbow Calibration Beads
71 (Biolegend). Gating strategies are presented in Supplemental Figure 1. Following
72 recommendations of the EuroFlow consortium, Panel 1 gives an overview of main adaptive
73 immune cell populations and memory formation in T and B cell subsets, using a double-staining
74 approach for markers specific to B and T cells(6). Panel 2 assesses the frequencies of thymic
75 output (recent thymic emigrants) and the proportion of T cells expressing the activation marker
76 HLA-DR. Furthermore, it enables comparison of two complementary gating strategies for T cell
77 subsets (based on CD27 and CD45RO or based on CCR7 and CD45RO). Panel 3 measures
78 the polarization status of memory T helper cells using expression patterns of surface
79 chemokine receptors that have been linked to expression of marker cytokines upon *ex vivo*
80 stimulation(7-9). Although low in frequencies, we excluded circulating T follicular helper (cTFH)

81 cells and the equivalent subset among Tregs (circulating T follicular regulatory (cTFR) cells)
82 by gating on CD45RO+CXCR5- T helper cells and Tregs for a more stringent analysis. The
83 presented analysis strategy enables comparable assessments of adaptive immunity cell
84 subsets in the small volumes of whole blood samples (e.g. 50-100 μ l for the 3 panels) available
85 for preterm infants without the need for cell isolation or freezing.

86 Statistical Analysis

87 Statistical analyses and graphical representations were performed using R software (version
88 4.4.3). In the *Immune Profiling Cohort*, outliers within lymphocyte subsets, defined as z-scores
89 < -3.29 or > 3.29 , were excluded prior to analysis. Group differences were assessed using
90 one-way ANOVA. In the *Extended Phenotype Cohort* due to smaller sample sizes and analysis
91 in subgroups group differences were assessed using Kruskal-Wallis test. Pairwise subgroup
92 comparisons were conducted using the Wilcoxon rank sum test with Benjamini-Hochberg
93 correction for multiple testing. Developmental trajectories of lymphocyte subset counts were
94 modeled using the Loess method implemented in the `geom_smooth` function. Missing data
95 were not imputed.

96 Principal component analysis (PCA) was conducted with the `prcomp` function (stats package)
97 with scaling to unit variance. Results were visualized using the `factoextra` (version 1.0.7)
98 package and `ggplot2` (version 3.5.1). Complete datasets from the *Immune Profiling Cohort*,
99 including lymphocyte counts and T-, B-, and NK-cell frequencies, were used for PCA.

100 `MetadeconfoundR` (version 1.0.2, <https://github.com/TillBirkner/metadeconfoundR>) was
101 employed to evaluate potential confounding effects of clinical metadata on lymphocyte subset
102 frequencies. The tool employs univariate statistics to identify associations between lymphocyte
103 subsets and sample metadata, subsequently applying nested linear model comparisons to
104 account for confounding effects(10). To minimize potential bias resulting from the fact that the
105 number of measurements obtained at later postnatal ages was higher in more premature
106 infants, we restricted the multivariate analyses to samples collected within the first 35 days of
107 life. AIS, sex, SGA, delivery mode, multiple birth, EOS, LOS, NEC, FIP, BPD, and IVH were

108 used as binary variables. Where appropriate, categorical variables were adapted to binary
109 classifications (e.g., clinical suspicion and histologically confirmed AIS were combined as AIS).
110 Prematurity (calculated in weeks to 40 weeks of gestation, where higher values indicate greater
111 prematurity) and birth weight (grams) were included as continuous variables. Associations and
112 confounding effects were analyzed separately for each postnatal age group.

113

114 SUPPLEMENTAL FIGURES

115 Supplemental Figure 1 – Flow cytometric gating strategies in *Extended Phenotyping Cohort*

116 Exemplary depiction of flow cytometric gating and analysis strategies used in FACS panel 1-
117 3. Resulting populations are named. Th: T helper cell; Tcon: conventional T cell; Treg:
118 regulatory T cell; cTFH: circulating T follicular helper cell; cTFR: circulating T follicular
119 regulatory cell, TEMRA: Effector memory T cells re-expressing CD45RA; RTE: Recent thymic
120 emigrants.

121 Supplemental Figure 2 – Immunophenotypes do not converge due to postmenstrual age

122 **A** Boxplots of PC1 values from the PCA (Figure 1 and this figure) grouped by postnatal time
123 of sampling and gestational age at birth. Each point represents an individual sample.
124 Significance was determined using one-way ANOVA to compare subset frequencies between
125 gestational age groups for a given range of time; ns: not significant, ***: $p < 0.001$, ****:
126 $p < 0.0001$. **B** Relative contributions of immune cell subsets used for PCA to principal
127 components 1 and 2. Positively contributing variables are shown in violet, negatively
128 contributing in petrol. **C** PCA representations of cellular immunophenotyping in preterm infants
129 in the first 49 days of life as in Figure 1 colored for gestational age at birth (weeks). Plots are
130 splitted for different postmenstrual ages (days). Each small circle represents an individual
131 sample, each large circle the geometric mean of all samples in the indicated gestational age
132 group within each plot (calculated when more than 10 measurements were available). PCA:
133 principal component analysis; PC: principal component; GA: gestational age.

134 Supplemental Figure 3 – Postnatal trajectories of lymphocyte and subset counts

135 **A-F** Lymphocyte and lymphocyte subset counts in peripheral blood of preterm infants grouped
136 for different gestational ages at birth in the first 49 days of life. Line indicates smoothed
137 conditional mean computed by Loess method, grey area indicates 95 % confidence interval.

138 Supplemental Figure 4 – Time intervals for analysis of postnatal trajectories of lymphocyte and
139 subset counts

140 **A-F** Lymphocyte counts and lymphocyte subset frequencies in peripheral blood of preterm
141 infants grouped for different gestational ages at birth in the first 49 days of life. Line show
142 smoothed conditional mean computed by Loess method, grey area indicates 95 % confidence
143 interval. Vertical lines define chosen time intervals for further analysis.

144 Supplemental Figure 5 – Postnatal development of T cell frequencies and CD4/CD8 ratios

145 Boxplots of **A** T cell frequencies and **B** CD4/CD8 ratios in preterm infants grouped by
146 gestational age at birth and postnatal time of sampling. Each point represents an individual
147 sample. Significance was determined using one-way ANOVA to compare subset frequencies
148 between gestational age groups for a given range of time; ns: not significant, ****: $p < 0.0001$.

149 Supplemental Figure 6 – Prematurity, amniotic infection syndrome and sex shape postnatal
150 cell trajectories of the adaptive immune system

151 Heatmaps illustrating the results of integrated analysis of immune cell trajectories and clinical
152 metadata using MetadeconfoundR. Stars indicate 'deconfounded' effects, circles indicate
153 effects 'confounded' by other variables. Positive effect sizes are shown in red, negative in blue.
154 **A** shows correlations between cell subsets and clinical metadata at defined postnatal ages. **B**
155 shows the same data rearranged according to cell subsets. FIP: Focal intestinal perforation;
156 BPD: Bronchopulmonary dysplasia; AIS: Amniotic infection syndrome; EOS: Early-onset
157 sepsis; LOS: Late-onset sepsis; SGA: Small for gestational age; IVH: Intraventricular
158 hemorrhage.

159 Supplemental Figure 7 – Postnatal development of lymphocyte subsets due to AIS

160 Boxplots of indicated lymphocyte subset frequencies (**A-E**) and CD4/CD8 ratios (**F**) in preterm
161 infants with and without the diagnosis of AIS (red and blue respectively) grouped by gestational
162 age at birth and postnatal time of sampling. Each point represents an individual sample.
163 Significance was determined between infants with and without AIS within subgroups using
164 Wilcoxon test with Benjamini-Hochberg correction for multiple testing strategy; only adjusted p
165 values < 0.05 are shown; *: $p < 0.05$, **: $p < 0.01$, ***: $p < 0.001$.

166 Supplemental Figure 8 – Postnatal development of lymphocyte subsets due to sex

167 Boxplots of indicated lymphocyte subset frequencies (**A-E**) and CD4/CD8 ratios (**F**) in male
168 (red) and female (blue) preterm infants grouped by gestational age at birth and postnatal time
169 of sampling. Each point represents an individual sample. Significance was determined
170 between male and female infants within subgroups using Wilcoxon test with Benjamini-
171 Hochberg correction for multiple testing strategy; only adjusted p values < 0.05 are shown; *:
172 $p < 0.05$, **: $p < 0.01$, ***: $p < 0.001$.

173 Supplemental Figure 9 – Comparison of lymphocyte and subset counts in the *Immune*
174 *Trajectory Cohort* and the *Extended Phenotyping Cohort*

175 **A-F** Lymphocyte and lymphocyte subset counts in peripheral blood of preterm infants grouped
176 for different gestational ages at birth in the first 49 days of life as in Supplemental Figure 2.
177 Grey points represent individual measurements from the *Immune Trajectory Cohort*, red dots
178 individual measurements from the *Extended Phenotyping Cohort*

179 Supplemental Figure 10 – Predominant naïve B cell phenotype in preterm infants

180 **A-F** Lymphocyte subset frequencies and counts in peripheral blood of preterm infants grouped
181 for different gestational ages at birth in the first week of life and at day 28. P values indicate
182 significances determined by Kruskal-Wallis test to compare subset frequencies between
183 gestational age groups within sampling groups. Asterisks mark significant differences to the
184 gestational age group '23-25' at the given time point calculated using Wilcoxon rank sum test
185 adjusted with Benjamini-Hochberg correction for multiple testing; only significant adjusted p
186 values are shown; *: $p < 0.05$.

187 Supplemental Figure 11 – Predominant effector T cell phenotype in preterm infants

188 **A-F** Lymphocyte subset frequencies and counts in peripheral blood of preterm infants grouped
189 for different gestational ages at birth in the first week of life and at day 28. **A-B** and **C-D**
190 respectively represent different flow cytometric gating strategies for analysis of corresponding

191 naïve, effector and memory T cell populations using either CD45RO and CD27 or CD45RO
192 and CCR7 surface expression (Supplemental Figure 1). P values indicate significances
193 determined by Kruskal-Wallis test to compare subset frequencies between gestational age
194 groups within sampling groups. Asterisks mark significant differences to the gestational age
195 group '23-25' at the given time point calculated using Wilcoxon rank sum test adjusted with
196 Benjamini-Hochberg correction for multiple testing; only significant adjusted p values are
197 shown; *: p<0.05, **: p<0.01.

198 Supplemental Figure 12 – Memory cell frequencies among CD4⁺ T helper cells and
199 conventional (non Treg) CD4⁺ T helper cells

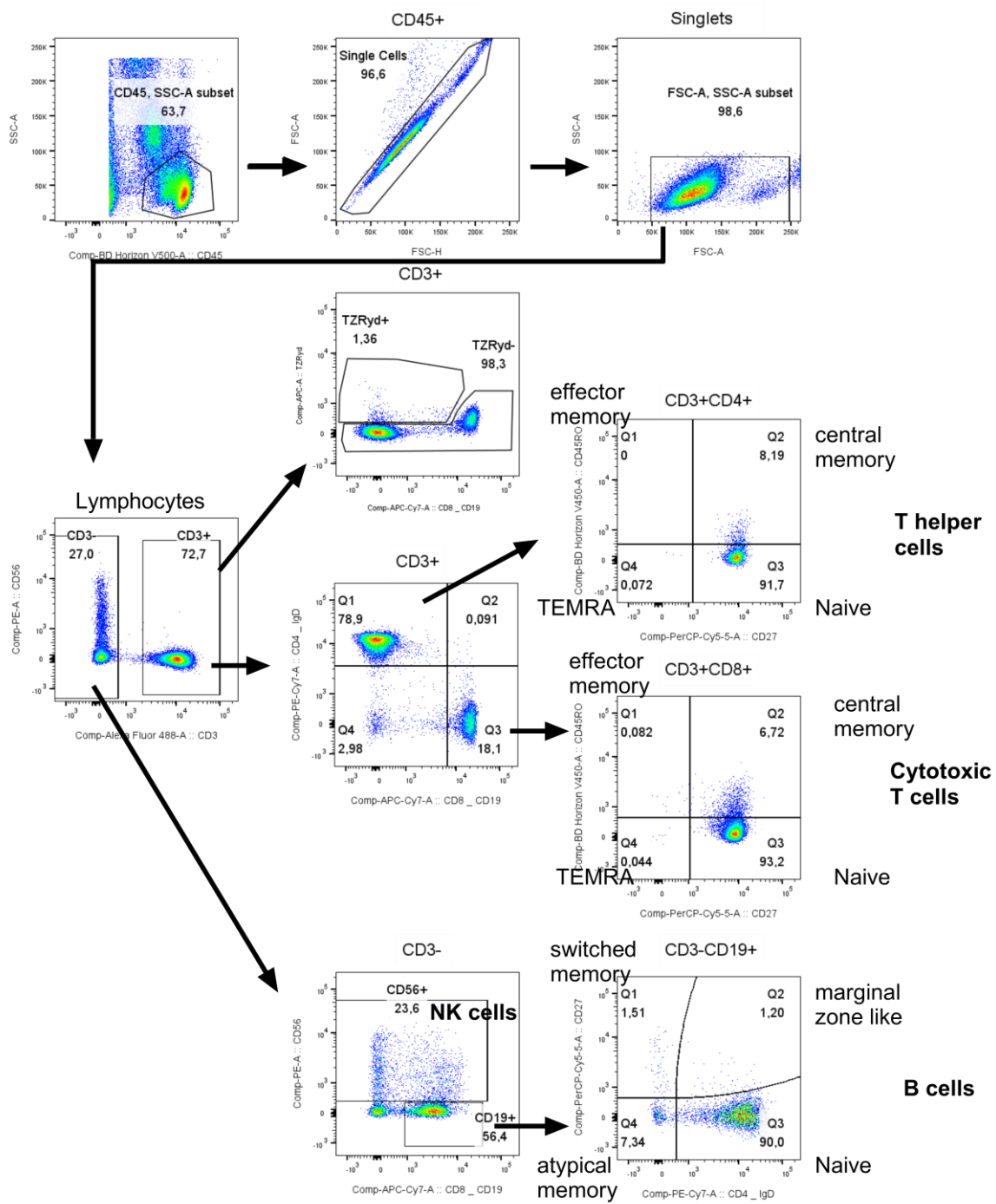
200 **A-B** CD45RO⁺CD4⁺ T helper and CD45RO⁺conventional (non Treg) CD4⁺ T helper cell
201 frequencies of CD4⁺ T cells in peripheral blood of preterm infants grouped for different
202 gestational ages at birth in the first week of life and at day 28. Significances were determined
203 as in Supplemental Figure 8 and 9.

204 Supplemental Figure 13 – Comparison of lymphocyte subset counts to published reference
205 values for SCID-screening

206 **A-F** Cell counts of lymphocytes and indicated lymphocyte subsets according to postmenstrual
207 age at time of blood draw. Every dot represents an individual measurement from the *Immune*
208 *Trajectory Cohort* in this study. Pink rectangles represent the ranges between the 5th and 95th
209 percentile of the published reference ranges by Amatuni et al., 2019(11).

210 Supplemental Figure 14 – Comparison of lymphocyte subset frequencies to published
211 reference values for SCID-screening

212 **A-D** Frequencies of indicated lymphocytes subsets according to postmenstrual age at time of
213 blood draw. Every dot represents an individual measurement from the *Immune Trajectory*
214 *Cohort* in this study. Pink rectangles represent the ranges between the 5th and 95th percentile
215 of the published reference ranges by Amatuni et al., 2019(11).

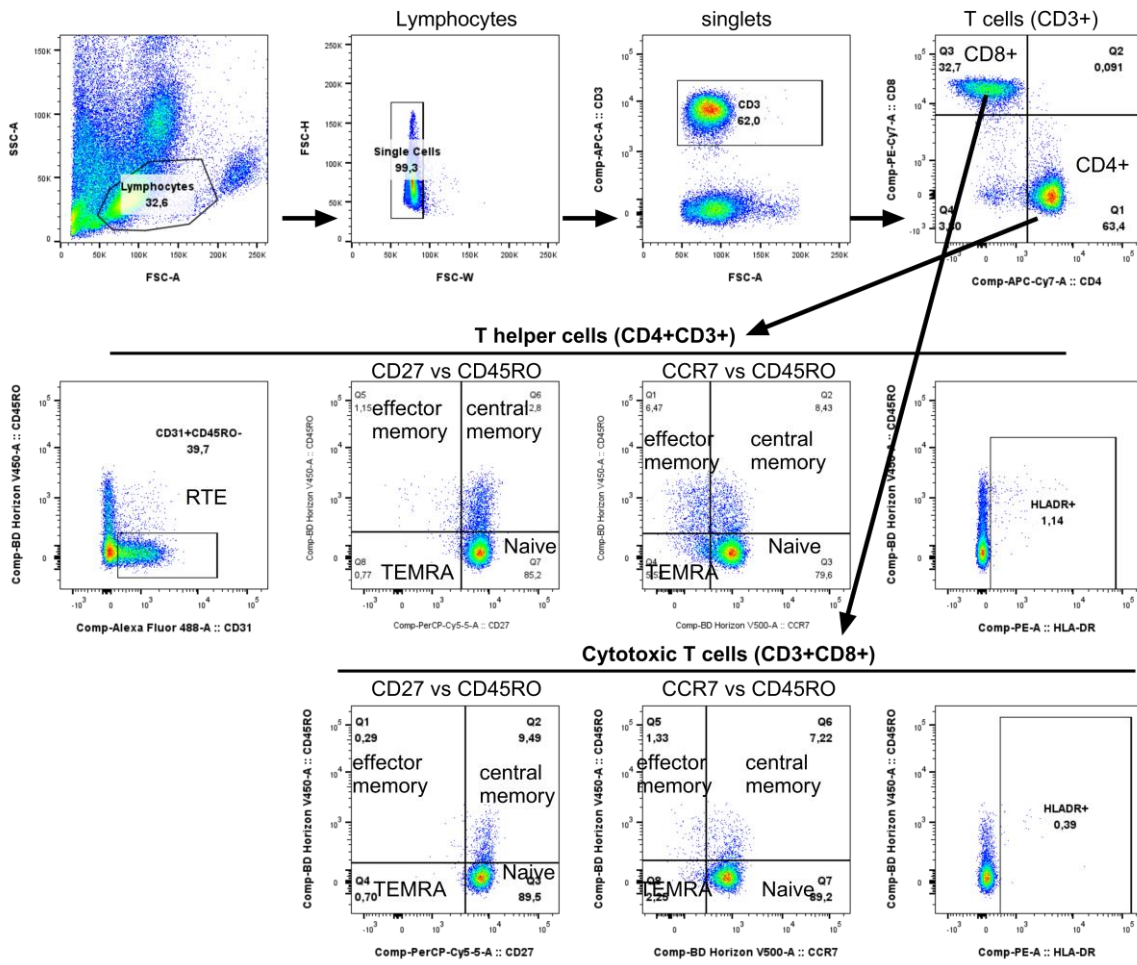


217

218

219

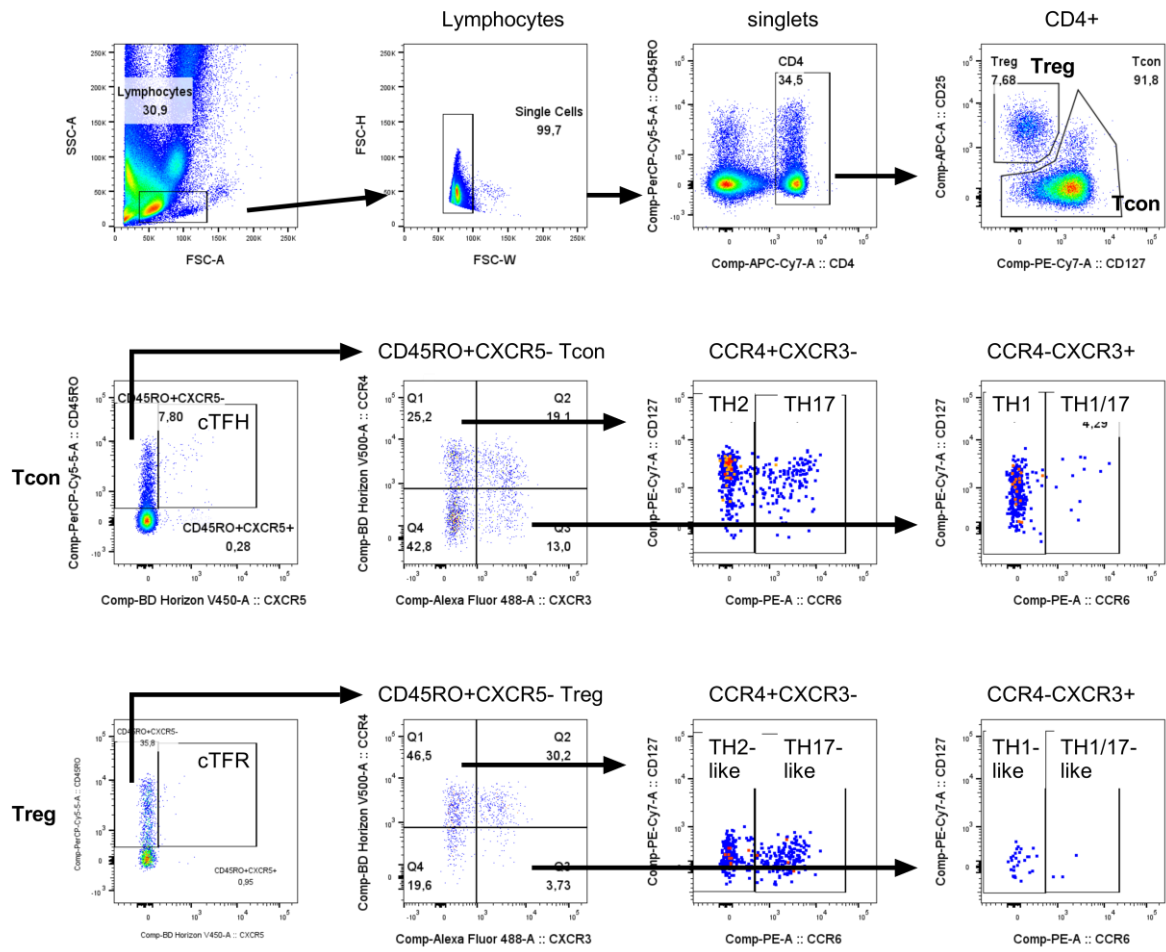
220 Supplemental Figure 1 – Panel 2



221

222

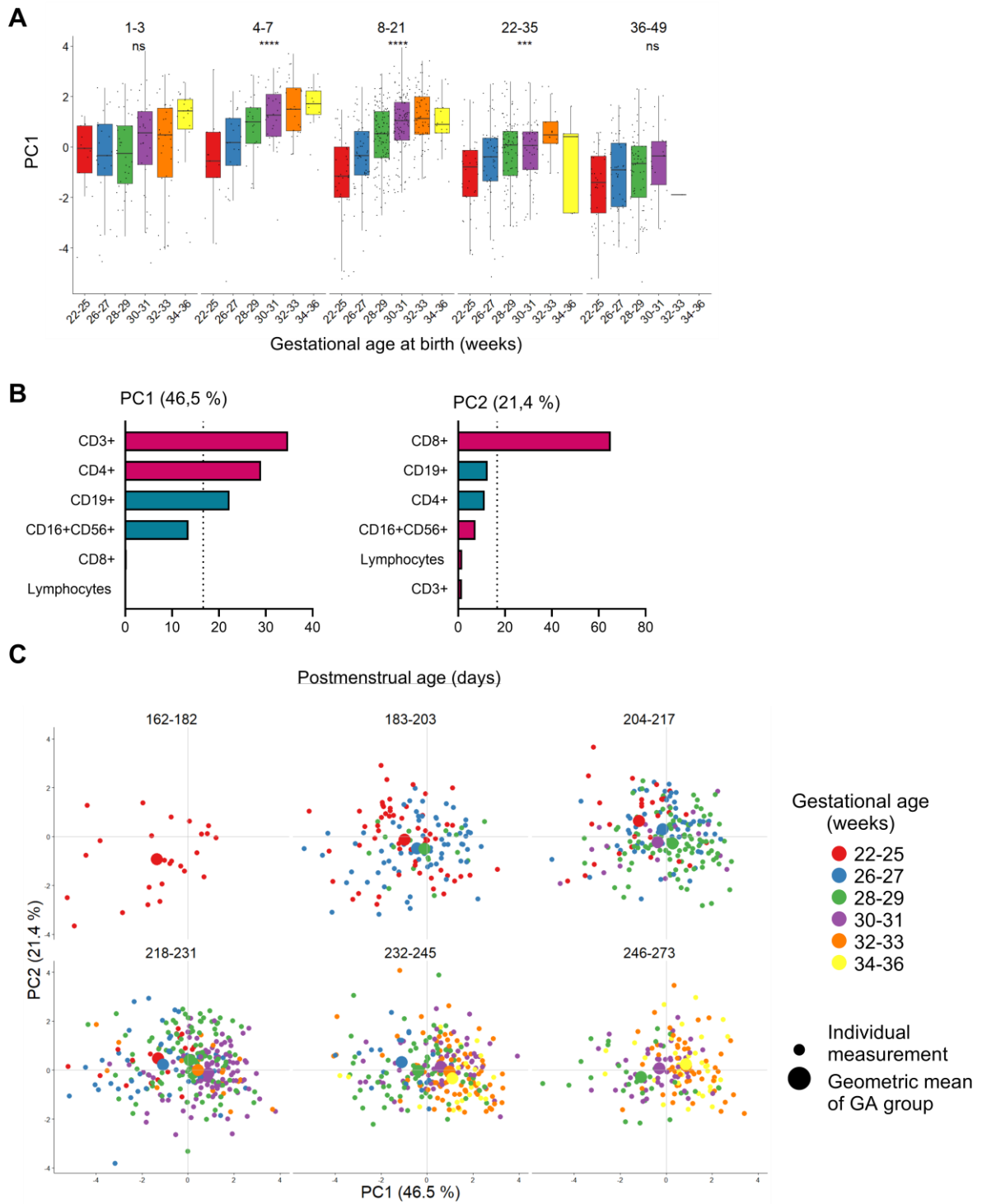
223



225

226

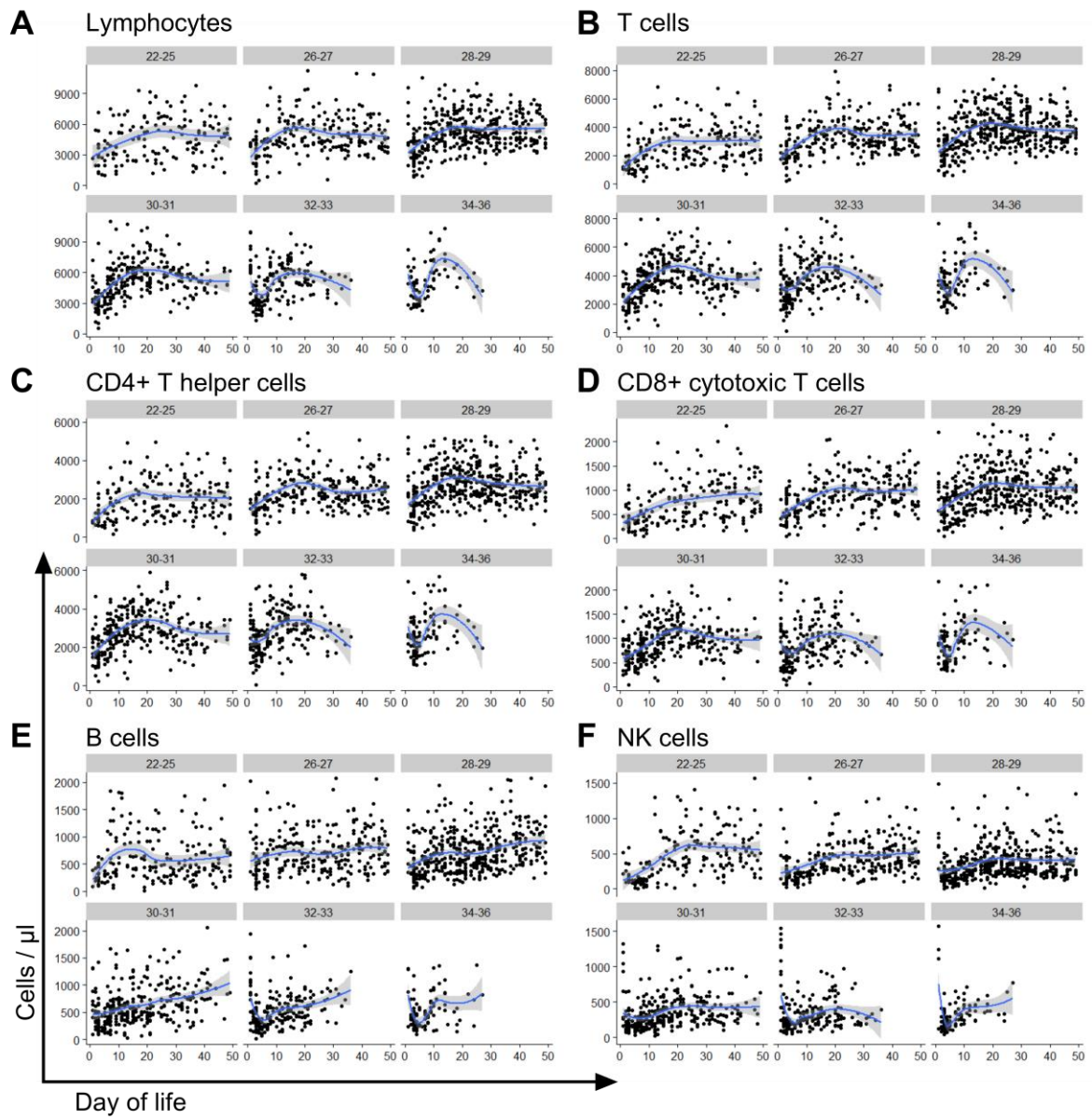
227



229

230

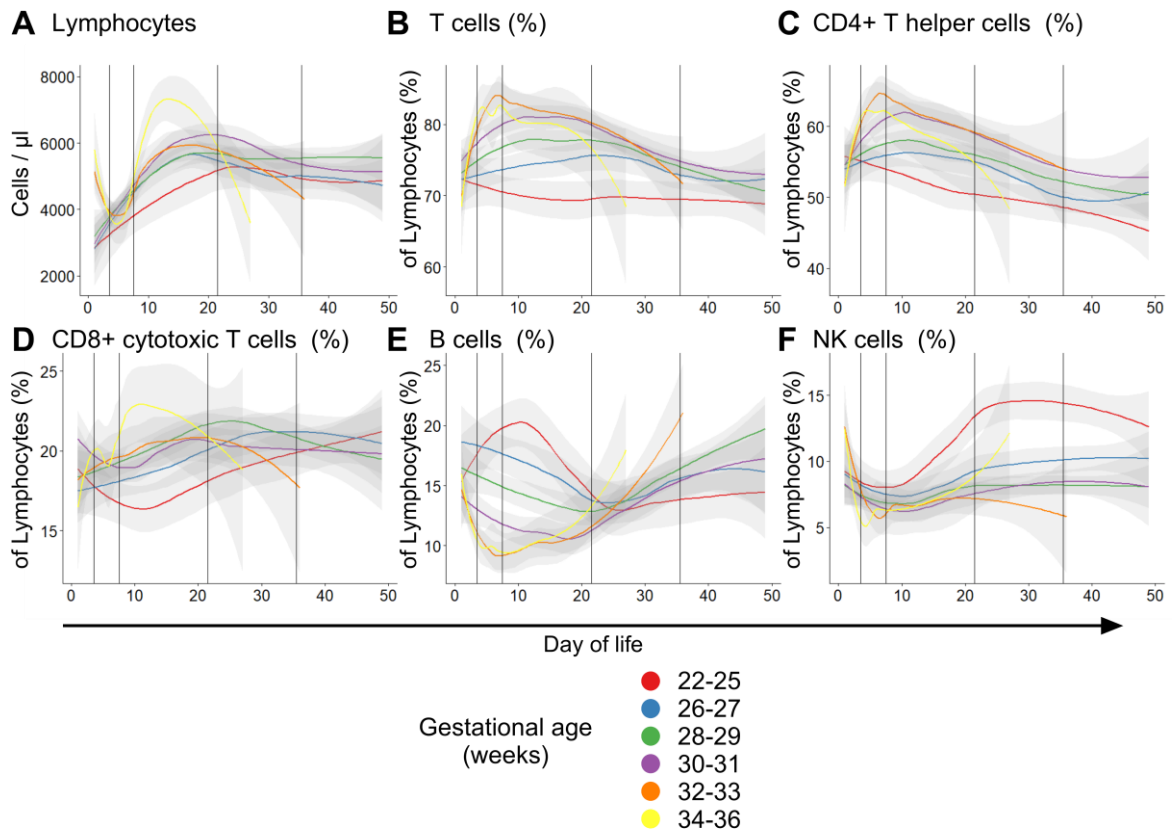
231



233

234

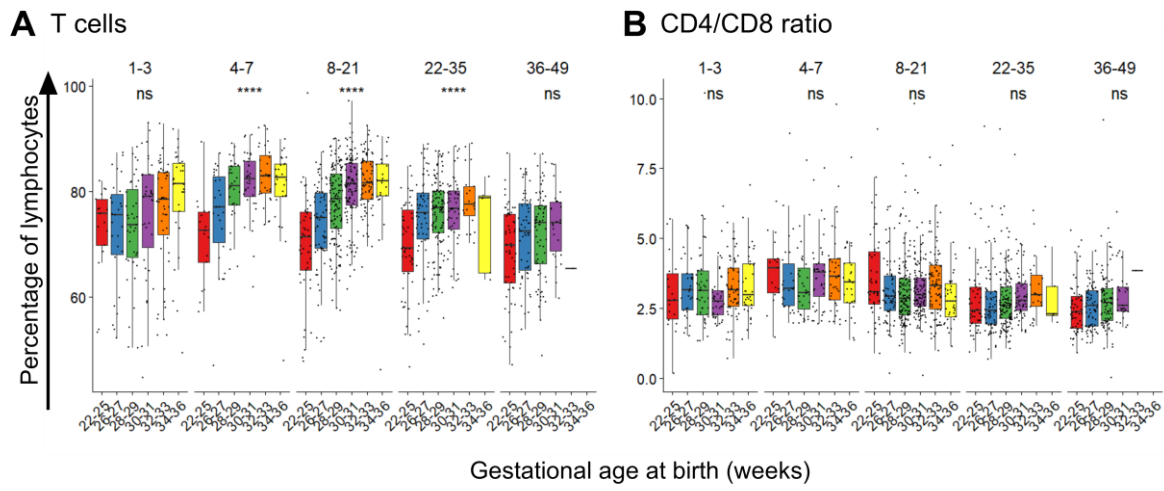
235



237

238

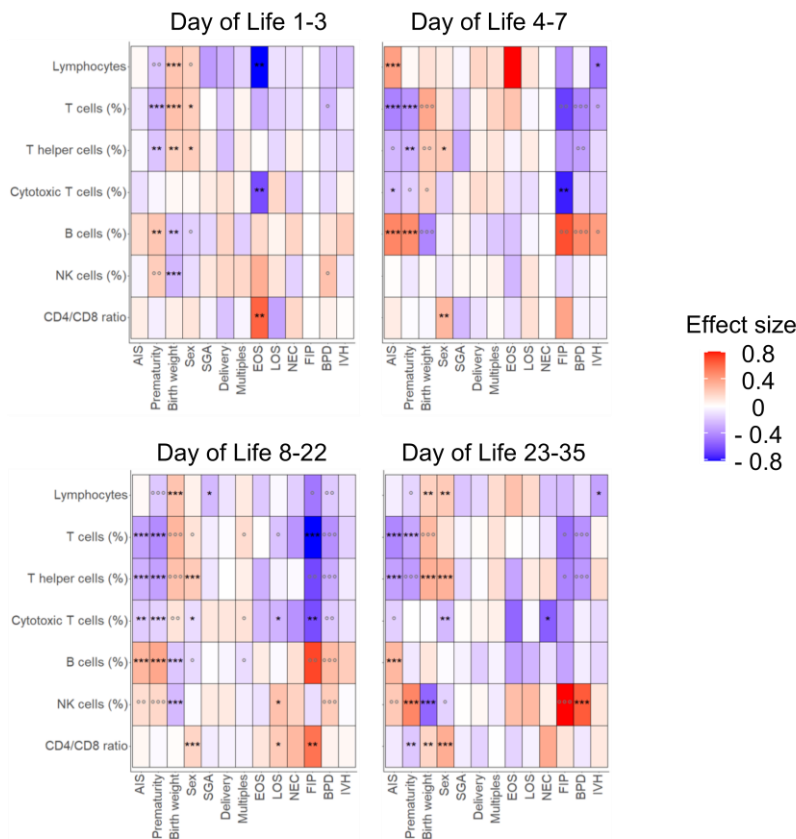
239



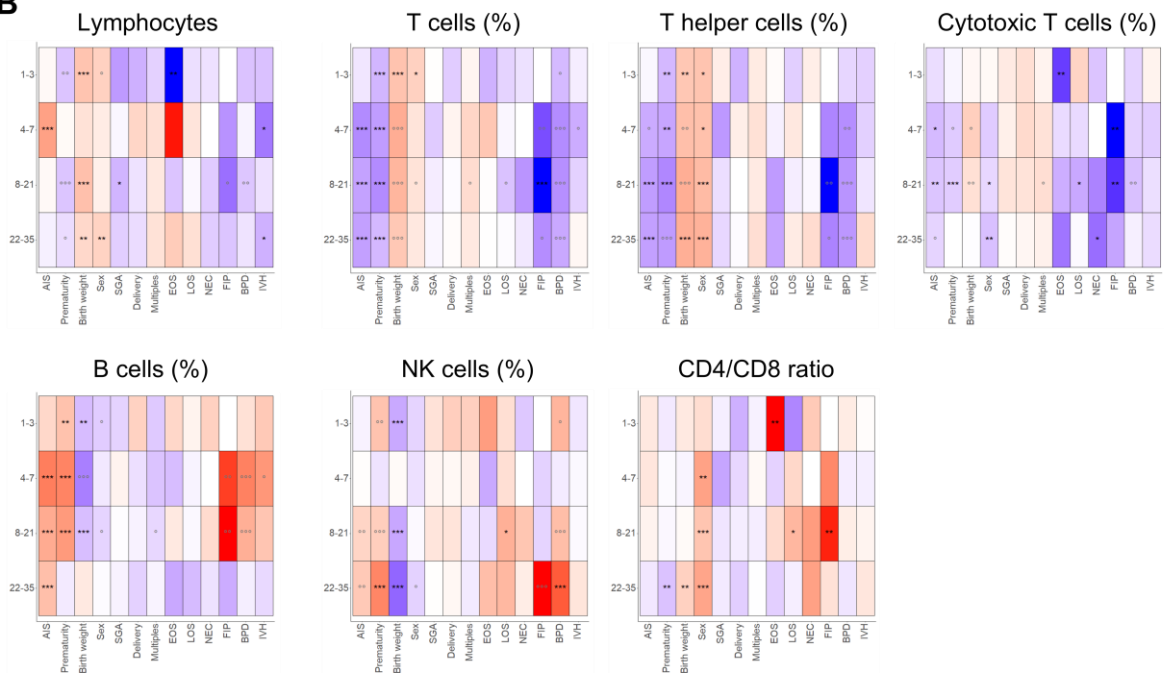
241

242

A



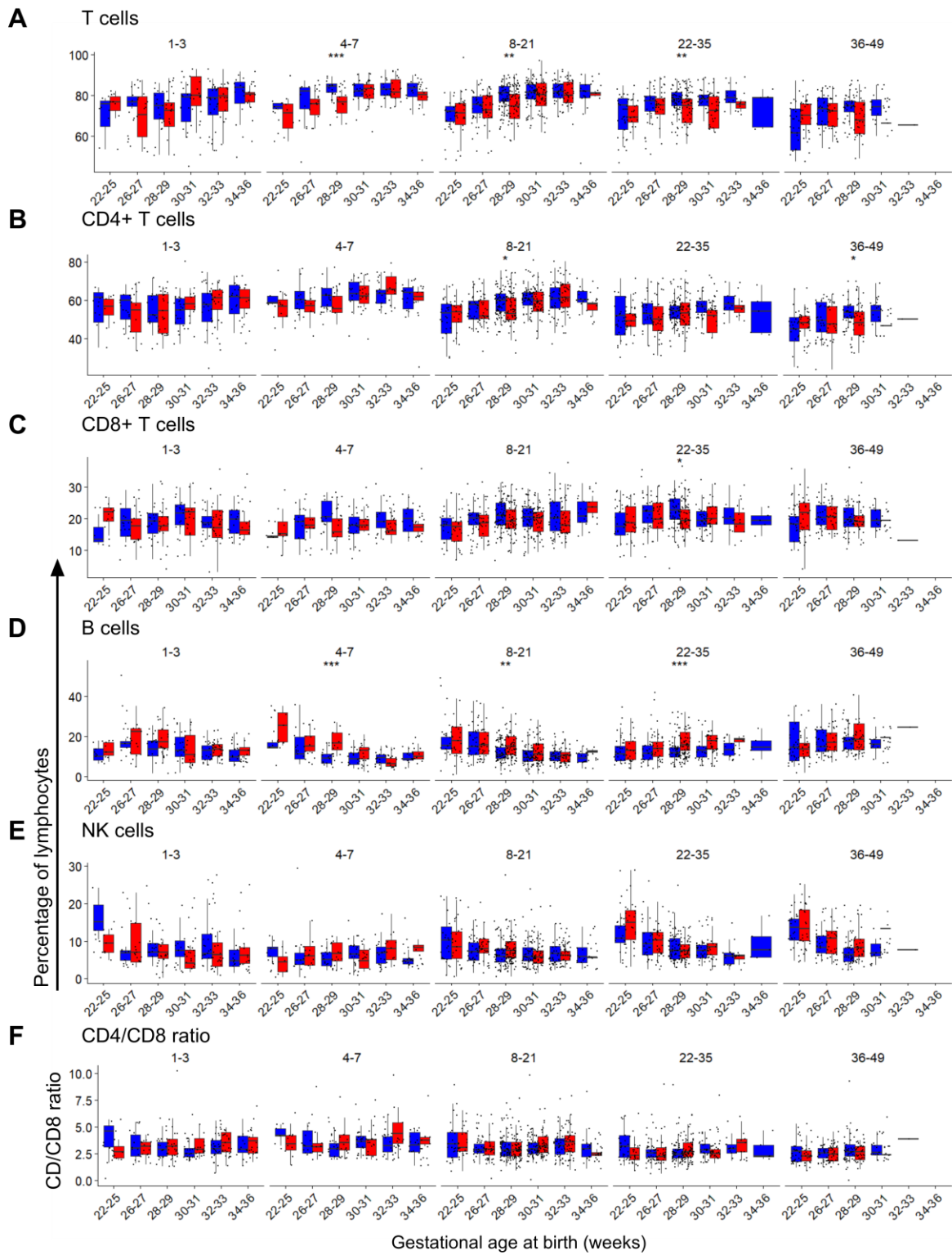
B



244

245

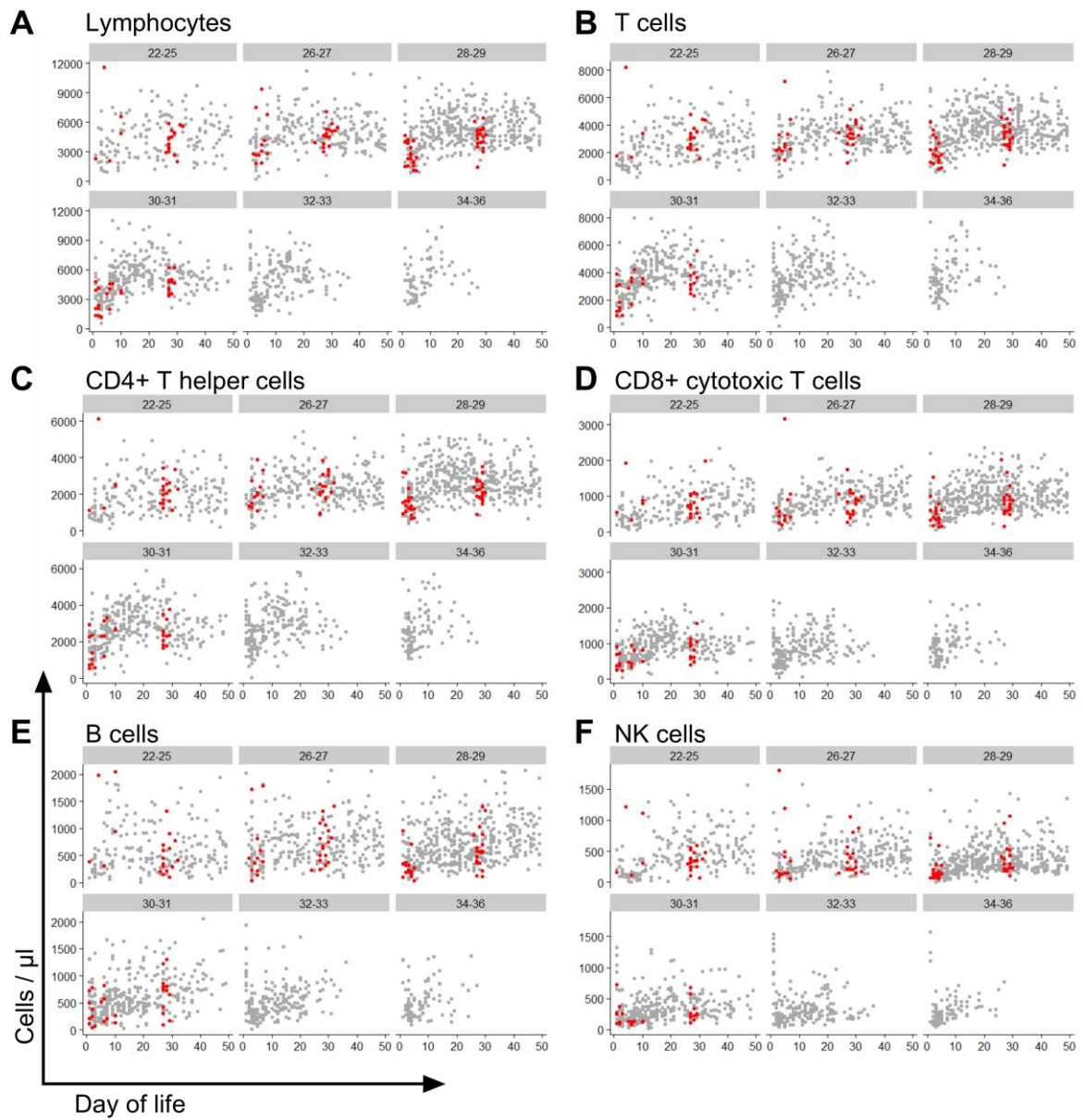
246



248

249

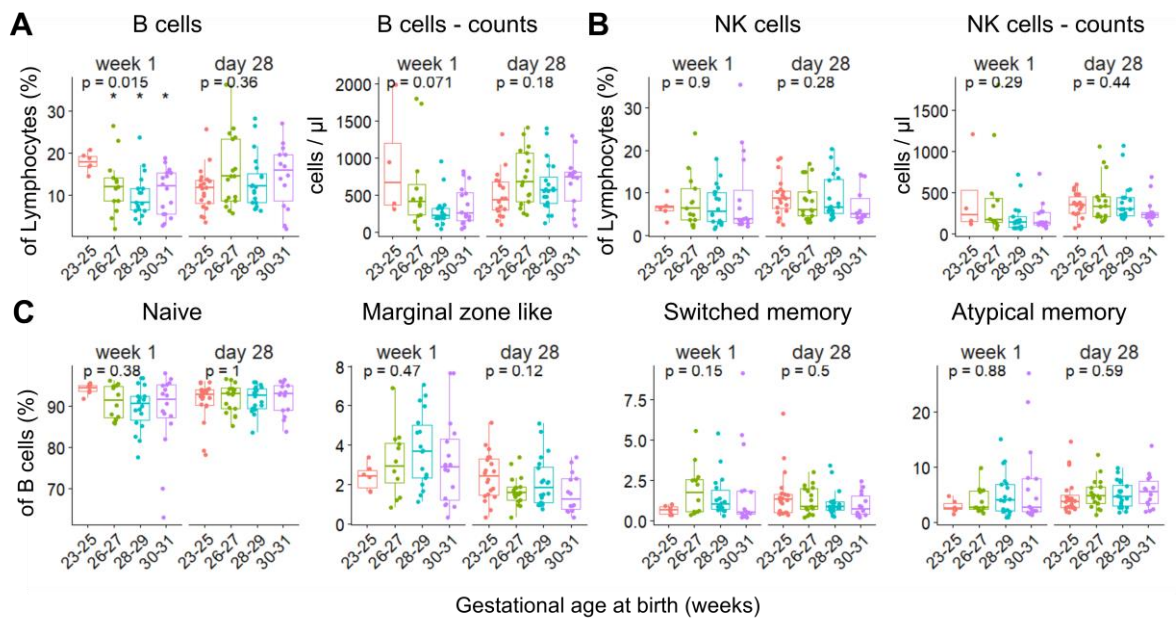
250



256

257

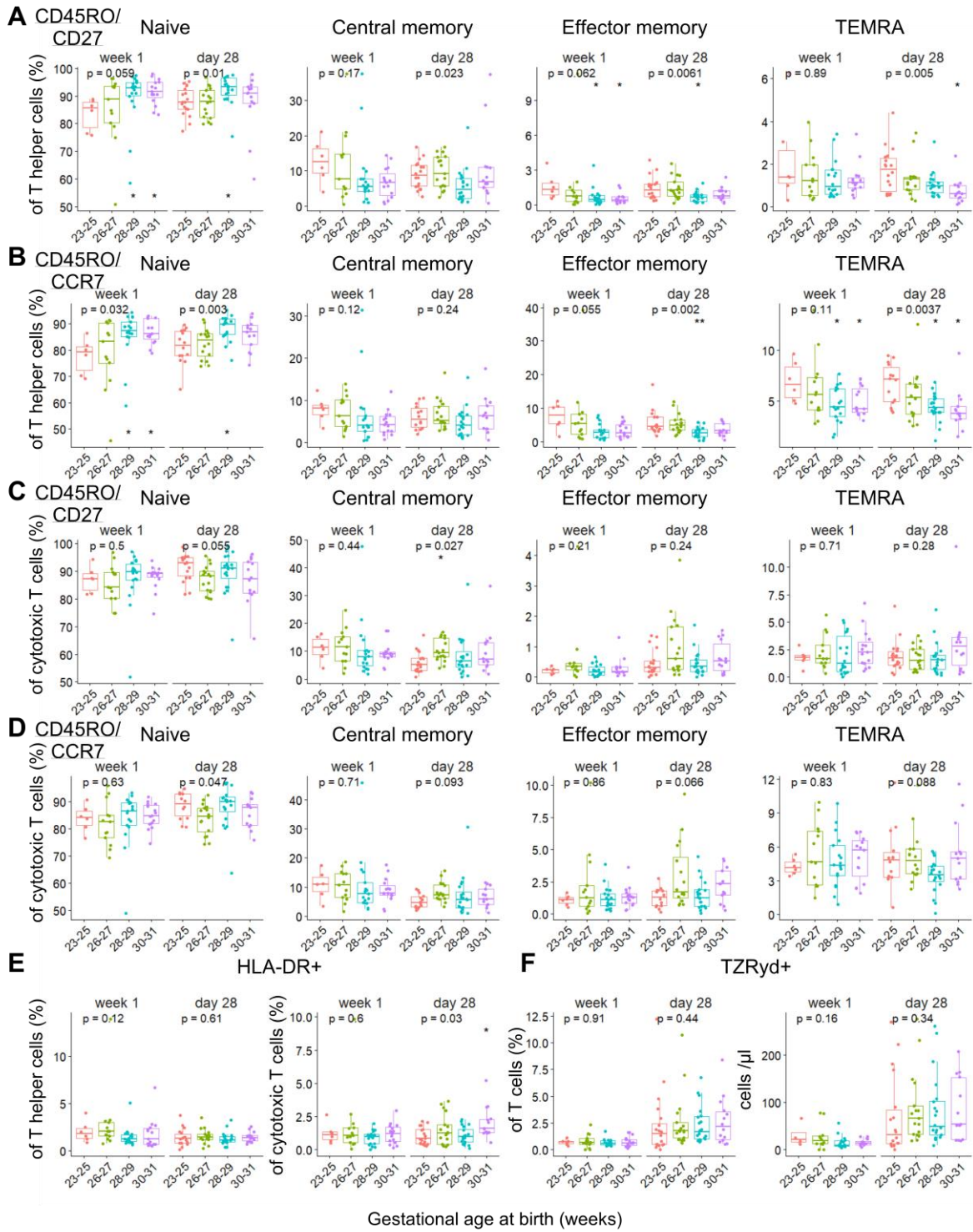
258



260

261

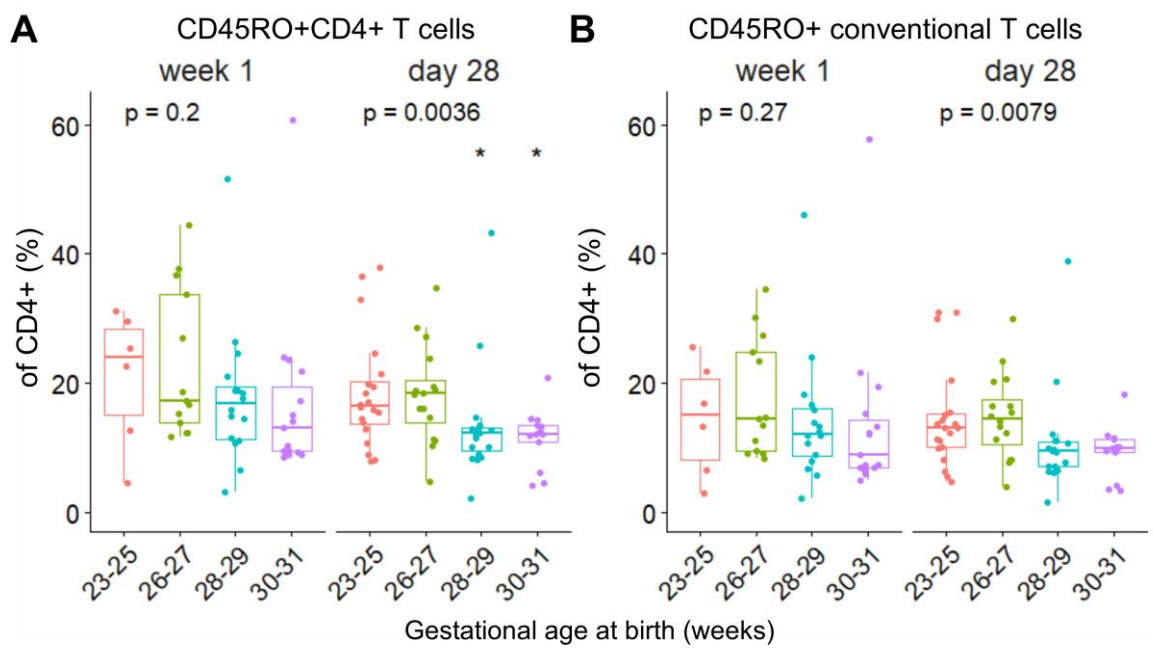
262



264

265

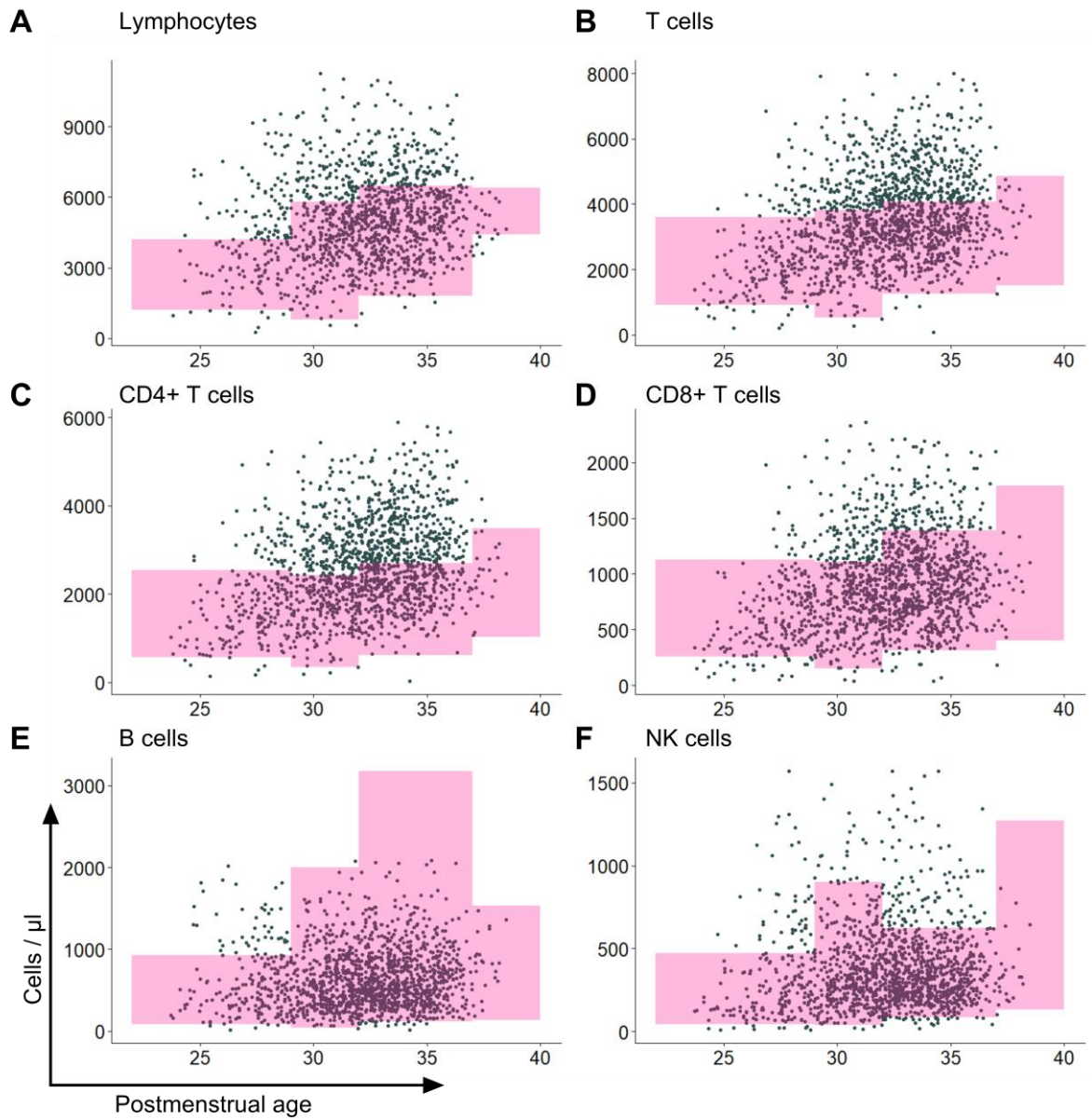
266



268

269

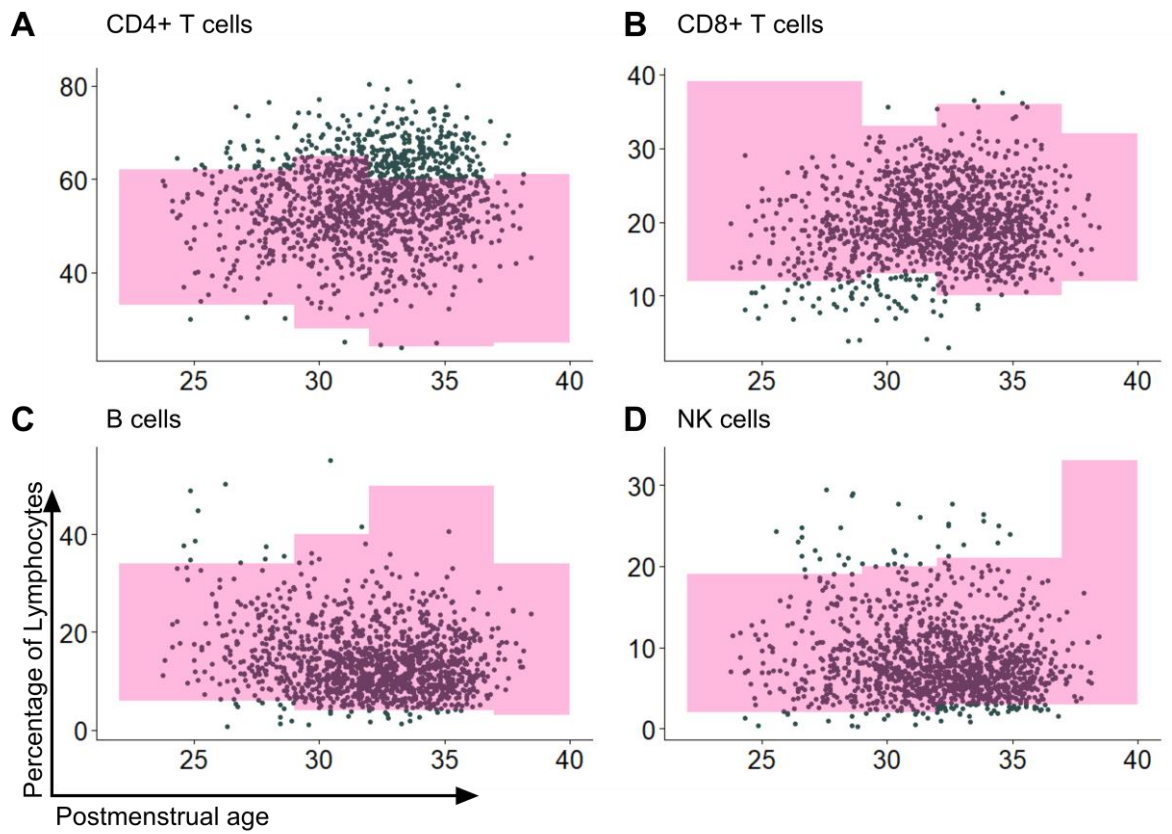
270



272

273

274



276

277

278

279 SUPPLEMENTAL TABLES

280 Supplemental Table 1

281 Clinical characteristics at birth of gestational age subgroups in the two cohorts. GA: gestational
282 age.

283 Supplemental Table 2

284 Monoclonal antibodies and fluorophores used for whole blood staining for flow cytometric
285 analysis of lymphocyte subsets. All antibodies used were from Biolegend.

286 **Supplemental Tables**

287

288 **Supplemental Table 1**

	Subgroup	22-25	26-27	28-29	30-31	32-33	34-36
Cohort 1	n	49	56	106	103	114	71
	GA at birth (median (range))	25 (22.9 - 25.9)	27.1 (26 - 27.9)	28.9 (28 - 29.9)	31 (30 - 31.9)	33 (32 - 33.9)	34.4 (34 - 36.4)
	Weight at birth (median (range))	680 (305 - 1100)	965 (385 - 1205)	1235 (600 - 1630)	1480 (665 - 2400)	1820 (1130 - 2645)	2190 (1270 - 2820)
	sex (% female)	34.7	46.4	52.8	59.2	54.4	42.3
Cohort 2	n	20	17	23	18	-	-
	GA at birth (median (range))	25.1 (23.9 - 25.9)	26.9 (26.1 - 27.9)	29.1 (28 - 29.9)	30.7 (30 - 31.9)	-	-
	Weight at birth (median (range))	640 (315 - 1055)	950 (590 - 1330)	1075 (395 - 1490)	1267.5 (720 - 1470)	-	-
	sex (% female)	40	55.8	56.5	44.4	-	-

289

290

291

Fluorochrome	Panel 1		Panel 2		Panel 3	
	Target	Clone	Target	Clone	Target	Clone
FITC	CD3	SK7	CD31	WM59	CXCR3	G025H7
PE	CD56	HCD56	HLA-DR	L243	CCR6	G034E3
APC	TZR $\gamma\delta$	B1	CD3	SK7	CD25	BC96
PerCP-Cy5.5	CD27	M-T271	CD27	M-T271	CD45RO	UCHL1
PE-Cy7	CD4	OKT4	CD4	OKT4	CD127	A019D5
	IgD	IA6-2				
APC-Cy7	CD8	SK1	CD8	SK1	CD4	OKT4
	CD19	HIB19				
BV421	CD45RO	UCHL1	CD45RO	UCHL1	CXCR5	J252D4
BV510	CD45	HI30	CD38	HIT2	CCR4	L291H4

294 REFERENCES

- 295 1. Voigt M, Rochow N, Straube S, Briese V, Olbertz D, Jorch G. Birth weight percentile charts
296 based on daily measurements for very preterm male and female infants at the age of 154-223 days. *J*
297 *Perinat Med.* 2010;38(3):289-95.
- 298 2. Schwab F, Gastmeier P, Piening B, Geffers C. The step from a voluntary to a mandatory
299 national nosocomial infection surveillance system: the influence on infection rates and surveillance
300 effect. *Antimicrob Resist Infect Control.* 2012;1(1):24.
- 301 3. Jobe AH, Bancalari E. Bronchopulmonary dysplasia. *Am J Respir Crit Care Med.*
302 2001;163(7):1723-9.
- 303 4. Papile LA, Burstein J, Burstein R, Koffler H. Incidence and evolution of subependymal and
304 intraventricular hemorrhage: a study of infants with birth weights less than 1,500 gm. *J Pediatr.*
305 1978;92(4):529-34.
- 306 5. Bell MJ. Neonatal necrotizing enterocolitis. *N Engl J Med.* 1978;298(5):281-2.
- 307 6. van der Burg M, Kalina T, Perez-Andres M, Vlkova M, Lopez-Granados E, Blanco E, et al. The
308 EuroFlow PID Orientation Tube for Flow Cytometric Diagnostic Screening of Primary
309 Immunodeficiencies of the Lymphoid System. *Front Immunol.* 2019;10:246.
- 310 7. Acosta-Rodriguez EV, Rivino L, Geginat J, Jarrossay D, Gattorno M, Lanzavecchia A, et al.
311 Surface phenotype and antigenic specificity of human interleukin 17-producing T helper memory
312 cells. *Nat Immunol.* 2007;8(6):639-46.
- 313 8. Sallusto F, Lanzavecchia A. Heterogeneity of CD4+ memory T cells: functional modules for
314 tailored immunity. *Eur J Immunol.* 2009;39(8):2076-82.
- 315 9. Zhang R, Miao J, Zhang K, Zhang B, Luo X, Sun H, et al. Th1-Like Treg Cells Are Increased But
316 Deficient in Function in Rheumatoid Arthritis. *Front Immunol.* 2022;13:863753.
- 317 10. Forslund SK, Chakaroun R, Zimmermann-Kogadeeva M, Marko L, Aron-Wisnewsky J, Nielsen
318 T, et al. Combinatorial, additive and dose-dependent drug-microbiome associations. *Nature.*
319 2021;600(7889):500-5.
- 320 11. Amatuni GS, Sciortino S, Currier RJ, Naides SJ, Church JA, Puck JM. Reference intervals for
321 lymphocyte subsets in preterm and term neonates without immune defects. *J Allergy Clin Immunol.*
322 2019;144(6):1674-83.

323